Resonance Measurement of Single- and Coupled-Microstrip Propagation Constants

VITTORIO RIZZOLI

Abstract—**The application of resonant techniques to the measurement of microstrip-line propagation constants is described. A review of the basic theory is given first, showing the great generality of the underlying principle. Then the particular case of a transmission line is discussed and it is shown that excellent theoretical accuracy can be achieved despite the simplicity of the procedure and the mathematics involved. Both the cases of nondispersive and dispersive propagation are covered. Finally, it is shown that the basic method can be extended to the case of symmetrical coupled lines in a straightforward way. Some results concerning practical microstrip lines are presented and compared with theoretical data.**

I. Introduction

RESONANT techniques are very popular among microwave engineers, as is shown by the considerable number of papers dealing with this subject that have been reported in literature. Though originally devoted to waveguide measurement (see, for example, [1]-[3]), these techniques have been successfully extended to the field of microwave integrated circuits [4]-[7]. In the latter case, many parameters of interest such as microstrip propagation constants, attenuation factors, and discontinuity equivalent circuits can be measured provided that resonators be suitably shaped and excited. In fact, the wide range of application seems to be one of the most attractive features of this kind of technique, the others being measurement simplicity and accuracy, easy automation, and insensitivity to such classical inconveniences of microstrip measurements as coaxial-to-microstrip transition effects.

This paper is concerned with propagation-constant measurement on single- and coupled-microstrip lines (or transmission lines in general). The theory of resonance measurement on one-port networks is reviewed in Section II in such a way that the extreme generality of the basic concept is emphasized. In Section III the application to measurement of single transmission-line propagation constants is discussed with the twofold aim of establishing the theoretical merits and limitations of the method and bringing into sharper focus some aspects that have been only partly covered so far. In Section IV it is shown that the measurement of the normal (i.e., even and odd)-mode propagation constants in a pair of symmetrical coupled transmission lines can always be reduced to a couple of independent single-transmission-line measurements. Interactions between different but nearby resonances are avoided this way and both modes are measured with the same absolute accuracy as obtained in the single-line case. Finally, in Section V a few experimental results are presented and compared with theoretical data in order to get a feeling of the kind of accuracy that can be expected from currently available analytical techniques in predicting microstrip behavior.

Manuscript received March 15, 1976; revised July 21, 1976. This work was sponsored by the Italian National Research Council (CNR). Part of this work was presented at the 1975 IEEE MTT-S International Microwave Symposium.

The author is with the Istituto di Elettronica, University of Bologna, Villa Griffone 40044 Bologna, Italy.

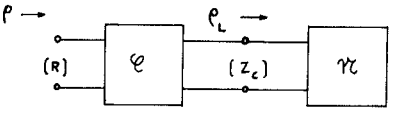

Fig. 1. Basic resonant configuration.

In any case reference is made to shielded line resonators, since this configuration has been shown [6] to be most suitable for obtaining accurate and well defined measurements and simply allows the even- and odd-mode resonances in the coupled case to be produced separately [9].

II. Resonance Measurement of One-Port Networks

The basic circuit configuration to be considered is shown in Fig. 1. The lossy one-port network under test $\mathcal{N}$ is coupled to the outside world by means of a lossless reciprocal two-port $\mathcal{C}$, and the reflection coeficient ρ of the resulting one-port is measured with respect to some reference impedance R (typically, the characteristic impedance of a network-analyzer system). The reference impedance at the inner port of the coupling network is denoted by Z_c (usually $Z_c \neq R$). Let the normalized driving point admittance of $\mathcal{N}$ be denoted by

$$y_L = \frac{1 - \rho_L}{1 + \rho_L} \tag{1}$$

and the scattering matrix of $\mathcal{C}$ by

$$S = \begin{bmatrix} s_{11} & s_{12} \\ s_{12} & s_{22} \end{bmatrix}. \tag{2}$$

Then, the expression for the input reflection coefficient is given by the well-known formula

$$\rho = s_{11} + \frac{s_{12}^2 \rho_L}{1 - s_{22}\rho_L}. \tag{3}$$

By means of (1) and a few algebraic manipulations, (3) can be given in the following form:

$$\rho = \frac{y_L - \dfrac{\Delta - s_{11}}{\Delta + s_{11}}}{y_L + \dfrac{1 - s_{22}}{1 + s_{22}}} \cdot \frac{\Delta + s_{11}}{1 + s_{22}} \tag{4}$$

where $\Delta = \det S$. Now, since (2) is the scattering matrix of a loss-free network, from the conditions for absence of loss we obtain

$$s_{11} = u \exp [-j\phi]$$
$$s_{22} = u \exp [-j\psi]$$
$$s_{12} = \pm j\sqrt{(1 - u^2)} \exp \left[-j \frac{\phi + \psi}{2}\right] \quad (5)$$

where u,ϕ,ψ are real numbers and $0 \leq u \leq 1$. Note that in this case we have $\Delta = \exp [-j(\phi + \psi)]$, so that (4) becomes

$$\rho = \frac{y_L - a - jb}{y_L + a - jb} \exp [j\delta] \quad (6)$$

with

$$a = \frac{1 - u^2}{1 + u^2 + 2u \cos \psi}$$
$$b = \frac{-2u \sin \psi}{1 + u^2 + 2u \cos \psi}$$
$$\delta = -\phi + \psi - 2 \arctan \frac{\sin \psi}{u + \cos \psi}. \quad (7)$$

Finally, if the real and imaginary parts of y_L are put into evidence, namely, $y_L = x + jy$, (6) takes the form

$$\rho = \frac{r_0 + jt}{1 + jt} \exp [j\delta] \quad (8)$$

where

$$r_0 = \frac{x - a}{x + a}$$
$$t = \frac{y - b}{x + a}. \quad (9)$$

Equation (8) is the expression for the reflection coefficient that will be referred to in the rest of the paper.

Let us now assume that the network $\mathscr{C}$ provides *small coupling* between its input and output ports, that is,

$$1 - u^2 \ll 1. \quad (10)$$

In the limiting case $u = 1$, (5) yields $s_{12} = 0$, so that $|\rho| = |s_{11}| = 1$ independent of frequency. Thus when (10) holds, the magnitude of the input reflection coefficient will generally be very close to 1, except in the vicinity of those frequencies (if any) such that the following conditions be satisfied:

$$|t| \ll 1$$
$$|r_0| \ll 1. \quad (11)$$

In fact, (11) implies $|\rho| \ll 1$. These frequencies will be referred to as *resonant frequencies*. Thus we may state that one such frequency is characterized by a *resonant dip* occurring in the magnitude-of-ρ-versus-frequency plot. The optimum theoretical case (usually not practically realizable) is achieved when

$$t = 0$$
$$r_0 = 0. \quad (12)$$

In this case the network $\mathscr{C}$ is said to provide *critical coupling*. To verify (12) or—from a more realistic standpoint—(11), a degree of freedom should usually be available in the circuit. Typically, this can be obtained by means of a coupling network containing at least one variable parameter. If r_0 and δ were constants, (8) would represent a circle on the Smith chart, having its center at

$$\frac{1 + r_0}{2} \exp [j\delta]. \quad (13)$$

Now in most practical cases it is found that the input reflection coefficient actually depicts a circle (or, at least, a fraction of it) on the Smith chart in the vicinity of every resonant frequency (see [7], [8]) provided that the reference plane be properly chosen. Referring to (8), this means that in the vicinity of a resonant frequency ω_s the rate of change of r_0 and δ with frequency is usually negligible if compared to that of t. Thus for ω near to ω_s from (8) we get the following approximate expression:

$$\rho(\omega) \simeq \frac{r_0(\omega_s) + jq(\omega - \omega_s)}{1 + jq(\omega - \omega_s)} \exp [j\delta] \quad (14)$$

where

$$q = \left.\frac{\partial t}{\partial \omega}\right|_{\omega = \omega_s}. \quad (15)$$

In turn, (15) suggests the following expression for the loaded Q of the resonant one-port [9]:

$$Q_L = \frac{q\omega_s}{2}. \quad (16)$$

Note that when (12) hold, Q_L is the inverse of the fractional 3-dB bandwidth so that by monitoring $|\rho|$ versus frequency on a CRT display Q_L can easily be measured. Of course, the resonant frequency ω_s can be measured quite as easily, since a sharp minimum of $|\rho|$ occurs at this frequency. Thus (12) and (16) may be regarded as a system of three equations which make it possible to find up to three unknown parameters of the one-port network under measurement. When the network topology is known *a priori* on a physical ground, the unknown quantities may obviously be chosen as physically significant ones. Otherwise, they are best chosen to be electrical parameters of some lumped or distributed equivalent circuit. An example of the former situation will be given in the following section, where the case of a short-circuited transmission line is worked out in some detail.

III. Propagation-Constant Measurement in a Transmission Line

Let the network $\mathscr{N}$ (Fig. 1) be a short-circuited transmission-line section of given length l. The line characteristic impedance (which is the same as the output reference

impedance) is denoted by Z_c and the unknown propagation constant by $\gamma = \alpha + j\beta$. If this is the case, the normalized load admittance is given by $y_L = \coth \gamma l$, and

$$x = \frac{\sinh 2\alpha l}{\cosh 2\alpha l - \cos 2\beta l}$$

$$y = \frac{-\sin 2\beta l}{\cosh 2\alpha l - \cos 2\beta l}. \tag{17}$$

If an ideal admittance inverter of constant B_0 is used as the coupling network $\mathscr{C}$, then

$$u = \frac{1 - B_0^2 Z_c R}{1 + B_0^2 Z_c R}$$

$$\phi = \psi = 0 \tag{18}$$

so that an easily realizable condition for small coupling is $B_0^2 Z_c R \ll 1$. Moreover, from (7) we get

$$a = B_0^2 Z_c R \ll 1$$

$$b = \delta = 0. \tag{19}$$

As a consequence, the condition $t = 0$ is met at all frequencies such that $\cos 2\beta l = \pm 1$. When the upper sign holds, $x = \coth \alpha l$, which is usually much greater than 1 since all the transmission lines we are interested in are low-loss. At these frequencies the magnitude of ρ is then nearly equal to 1 and no resonance is found. Thus resonances may only occur at frequencies such that the line length is an odd multiple of a quarter of a wavelength, that is,

$$\omega_s = \frac{v_p}{l}(2K + 1)\frac{\pi}{2} \tag{20}$$

where K is an integer and v_p is the phase velocity of the transmission line. At all frequencies defined by (20), the input reflection coefficient is given by

$$\rho(\omega_s) = r_0 = \frac{\tanh \alpha l - B_0^2 Z_c R}{\tanh \alpha l + B_0 Z_c R} \tag{21}$$

and a resonant dip may actually occur provided that the inverter constant B_0 is properly adjusted. This is the degree of freedom required to perform the measurement in the particular case being considered.

Finally, from (16) by means of (15), (9), and (17) the following expression for the loaded cavity Q is derived:

$$Q_L = \frac{v_p}{v_g}\frac{(1 - \tanh^2 \alpha l)(2K + 1)\pi}{4(\tanh \alpha l + B_0^2 Z_c R)} \tag{22}$$

where

$$v_g = \frac{\partial \omega}{\partial \beta} \tag{23}$$

is the group velocity of the transmission line. Equations (20), (21), and (22) can be rearranged to obtain the fundamental equations for the measurement procedure:

$$v_p = \frac{2\omega_s l}{(2K + 1)\pi}$$

$$\tanh \alpha l = \sqrt{(Y^2 + 1)} - Y \tag{24}$$

$$B_0^2 Z_c R = \frac{1 - \tanh^2 \alpha l}{(1 + r_0)Y} - \tanh \alpha l$$

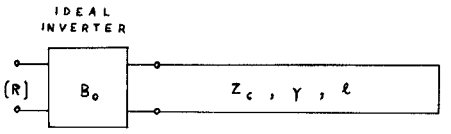

Fig. 2. Inverter-fed transmission-line resonant cavity.

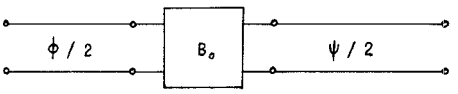

Fig. 3. Equivalent circuit of general lossless two-port.

where

$$Y = \frac{v_g}{v_p} \cdot \frac{4Q_L}{(2K + 1)\pi(1 + r_0)}. \tag{25}$$

In (24), Q_L, ω_s, and r_0 must be regarded as known quantities.[1] The network topology for this case is schematically shown in Fig. 2.

At this stage, two different cases may arise. When propagation in the line is nondispersive, then $v_p = v_g$ and (24) yield the phase velocity and attenuation constant of the line without further complication. When dispersion may not be neglected, further information is required to find the group velocity. This can be obtained on a purely experimental basis following the procedure outlined in the Appendix.

Now consider the two-port network represented in Fig. 3, made of two lossless transmission-line sections and an ideal admittance inverter. It is well known that this network can be used as an equivalent circuit for any loss-free two-port at a given frequency. Consequently, in the vicinity of every resonant frequency the real network may be described by the ideal topology of Fig. 2[2] *no matter what the physical structure of the coupling network*, provided that the following conditions are fulfilled:

1) the coupling network is practically loss free;
2) the output electrical length of the coupling network is negligible with respect to the electrical length of the line resonator.

Note that the input electrical length of the coupling network is of no interest here, since its effect can be easily compensated for by a reference plane shift.

Thus the fundamental equations for the ideal case may be used in the real situation as well, the only approximations involved being specified by conditions 1) and 2) above. In particular, it is expected that the relative error on v_p will be of the order of

$$\frac{\psi}{(2K + 1)\pi}. \tag{26}$$

[1] Note that (24) may be used even when $|r_0|$ is nonnegligible with respect to unity. In this case the loaded Q is defined as the ratio $\omega_s/\Delta\omega$, where $\Delta\omega$ is the difference between the two frequencies yielding $|\rho|^2 = (1 + r_0^2)/2$. The latter reduces to the 3-dB bandwidth if $r_0^2 \ll 1$.

[2] At least, this is true within the 3-dB bandwidth, which is usually very narrow (typically a few percent).

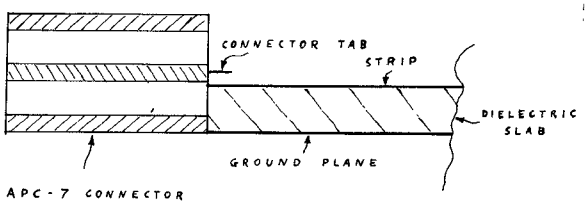

Fig. 4. Example of microstrip-cavity excitation.

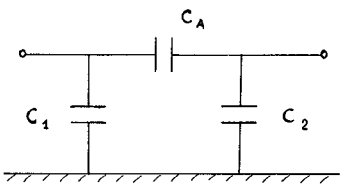

Fig. 5. Equivalent circuit of coupling network.

A very simple practical realization of the coupling network—in fact, the one that was used to perform the measurements presented in this paper—is schematically shown in Fig. 4. The network essentially consists of an air gap separating the output tab of an APC-7 RF connector and the input section of the microstrip line. The coupling can be made as small as needed by varying the gap. It is evident on a physical ground that this kind of network can be described by an equivalent circuit consisting of a purely capacitive π-network as shown in Fig. 5. C_1 and C_2 approximately account for the end effects of the coaxial and microstrip lines.

Since a number of approximations are involved in the above procedure, it is advisable to get some sort of feeling of the overall theoretical accuracy that can be expected from it. To this end, computer simulations were performed in a number of particular cases.

The way a simulation works is as follows. An analytical model of the microstrip resonator is assumed first, including dispersion [10], frequency-dependent losses and parasitics. All of these effects are taken into account by simple equations based on well-known theoretical or experimental data. Reasonable values are then chosen for C_1 and C_2 in a similar way [11]. At this stage, a value of K (order of resonance) is fixed and the corresponding resonance frequency and critical coupling capacitance are found by numerically solving (12). The resulting one-port is then analyzed and the magnitude of the reflection coefficient is plotted as a function of frequency. Finally, this plot is used (in much the same way as if it was the trace on a CRT display) to find the line propagation constant by the method previously described and the results are compared with the known true values.

Based on the data obtained this way, we can state that the theoretical accuracy of the method is higher than 2.5 percent in all cases of practical interest for a 5-cm-long resonator within the band 1:18 GHz.

Dispersion must be taken into account as approaching the upper end of this band. Increasing the resonator length usually increases both the accuracy on v_p and the error on α.

The case of an open-end resonator can be treated in a very similar way. The fundamental equations (24), (25) still hold, provided that the factor $(2K + 1)$ is replaced by $2K$. In this case the end effect of the microstrip line should be taken into account in evaluating the phase velocity. However, for resonator lengths over 5 cm this effect is usually less than a few units per thousand.

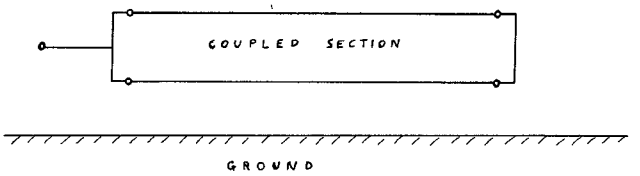

Fig. 6. Schematic of even-mode cavity.

Finally, note that the effect of any circuit losses other than the ones to be measured can easily be accounted for by shifting the vertical position of the beam on the CRT display in such a way that the out-of-resonance condition $|\rho| \simeq 1$ is restored. Then the measurement may be carried out in the way discussed so far without further complication.

IV. Resonance Measurement of Even- and Odd-Mode Propagation Constants in Coupled Microstrips

The method outlined in the preceding sections, which is suitable for single-transmission-line measurement, can be used in the case of symmetrical coupled microstrips to find the even- and odd-mode propagation constants. The approach consists of feeding and loading a section of the two-wire line to be measured in such a way that separate resonant cavities for the even and odd mode be obtained. The even- and odd-mode voltages and currents are defined by the well-known relationships

$$V_E = \frac{V_1 + V_2}{2} \qquad V_0 = \frac{V_1 - V_2}{2}$$

$$I_E = \frac{I_1 + I_2}{2} \qquad I_0 = \frac{I_1 - I_2}{2}. \tag{27}$$

An even-mode resonant cavity can very easily be obtained by connecting in parallel the strips at both ends of the coupled section as shown in Fig. 6. In this way we force the odd-mode voltage to be zero in both the input and load sections of the two-wire line. Since the modes are uncoupled in all other sections, the odd mode is not excited at all. As a consequence, a transmission-line resonator is obtained having the even-mode propagation constant γ_E and half the even-mode characteristic impedance. The input coupling network is realized as shown in Fig. 4 and an open-end configuration is chosen to simplify construction. The resonator is enclosed in a rectangular waveguide below cutoff in order to eliminate any radiation effects.

To obtain an odd-mode resonant cavity, let us first consider the electrical situation depicted in Fig. 7. The strips are connected in parallel at the input side, and separately loaded by the admittances Y_1, Y_2. This time the RF connector is soldered to the center conductor, so that no input admittance inverter exists. As shown in [9], the equivalent

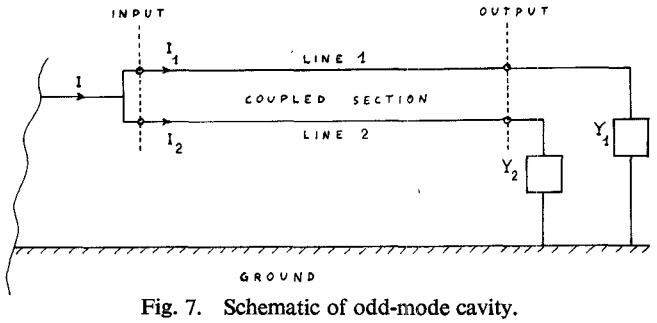

Fig. 7. Schematic of odd-mode cavity.

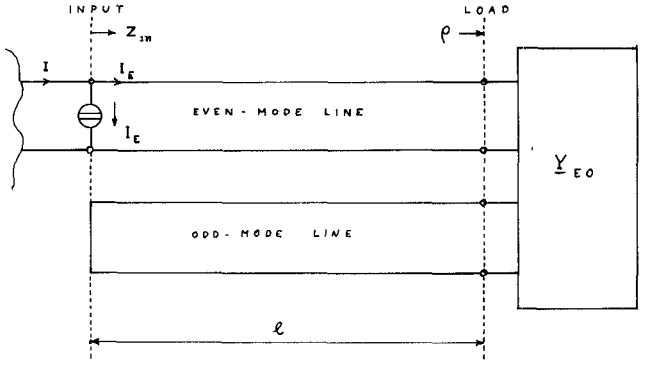

Fig. 8. Equivalent circuit in terms of even- and odd-mode transmission lines.

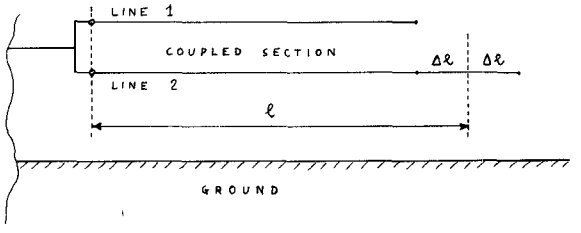

Fig. 9. Final configuration of odd-mode cavity.

circuit of Fig. 7 in terms of even- and odd-mode lines is the one given in Fig. 8. The two-port labeled Y_{E0} becomes an ideal admittance inverter of constant $B_0 \ll 1$ provided that

$$Y_1 = -jB_0$$
$$Y_2 = jB_0 \tag{28}$$

where B_0 is a small real number.

Due to the presence of a cascade section of the even-mode line, the electrical situation of Fig. 8 is somewhat more complicated than assumed in Section III, and must be carefully examined.

What we would need in order to perform the measurement as described above is the reflection coefficient of the odd-mode resonator *with respect to the even-mode characteristic impedance* (this is denoted by ρ in Fig. 7). On the other hand, what we are *able* to measure from the circuit of Fig. 7 is

$$\rho_{\text{in}} = \frac{\frac{1}{2}Z_{\text{in}} - R}{\frac{1}{2}Z_{\text{in}} + R} \tag{29}$$

where R is the reference impedance and Z_{in} is given by

$$Z_{\text{in}} = Z_E \frac{1 + \rho \exp[-2\gamma_E l]}{1 - \rho \exp[-2\gamma_E l]} \tag{30}$$

l being the length of the coupled section.[3]

Now since the loaded Q of the cavity is usually high, and we are essentially interested in the circuit behavior within the narrow 3-dB bandwidth, the change of the factor $\gamma_E l$ with frequency throughout this band may be neglected. Moreover, since the even mode is generally low loss (see Section V), the attenuation factor may be neglected, too, or simply accounted for as was said at the end of Section III. Thus the cascade even-mode line acts in much the same way as an ideal phase shifter in the frequency band of interest. If this is the case, it can be shown that a straightforward application of (24) to the measured reflection coefficient ρ_{in} (see Fig. 7) yields the correct value of the odd-mode propagation constant in spite of the impedance step occurring in the input section of the microstrip circuit. The approximation error involved is typically 1 percent or less in cases of practical interest. The proof of this statement is not given here for the sake of brevity.

The only problem left is how to obtain the practical realization of (28). An intuitive solution can readily be found if we note that a small positive susceptance can be made by a short ($< \lambda/4$) open-end transmission-line section, while a small negative susceptance could be made by a similar transmission-line section of *negative* length. Thus all we need [9] is to lengthen one of the strips and shorten the other by the same amount Δl. The resulting circuit configuration is schematically shown in Fig. 9. The inverter constant is given by

$$B_0 = Y_0 \tan \beta_0 \Delta l, \tag{31}$$

where Y_0 and β_0 are the characteristic admittance and phase constant of the open-circuited stub loading line 2. In principle, the inverter constant can be adjusted by changing the length Δl, so that the required degree of freedom is available.

Upon careful examination of the circuit in Fig. 9, it becomes evident that the above intuitive argument is only approximate. An exact equivalent circuit is actually given by Fig. 8, where l must be replaced by $l - \Delta l$ and the coupling network has the same topology as shown in Fig. 5. This time the equal capacitances $C_1 = C_2$ account for the microstrip open-circuit effect, while the coupling capacitance C_A has the expression

$$C_A = Y_0 \Delta l \frac{\beta_0}{\omega_s}. \tag{32}$$

[3] In principle, a very simple way of exactly solving the problem would be to make $R = Z_E/2$ by inserting an impedance-matching network between the microstrip circuit and the output connector of the network-analyzer system. In fact, in this case from (29) and (30), we get

$$\rho_{\text{in}} = \rho \exp[-2\gamma_E l]$$

so that ρ can be derived from the measured data, since γ_E is known. This approach, however, turns out to be unpractical because it requires an independent determination of the even-mode characteristic impedance and can be greatly perturbed by the imperfect behavior of the matching network.

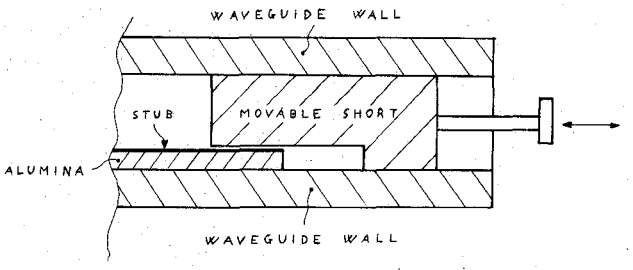

Fig. 10. Fine tuning of odd-mode cavity.

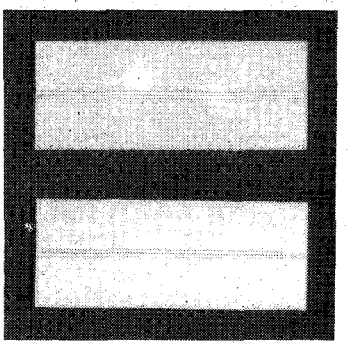

Fig. 11. Picture of even- and odd-mode cavities.

Thus the electrical situation and the expected accuracy are the same as that discussed in Section III for the single-line case.

Finally, note that, in order to practically perform the measurement, a fine tune of the inverter constant can be realized as shown in Fig. 10. As in the previous case, the resonator is enclosed in a rectangular waveguide below cutoff, but now a step is etched in the shorting block delimiting the waveguide cavity. The length of this step is the same as for the stub loading line 2, and the height is such that a very small air gap ($\simeq$ 0.1 mm) is left between the strip conductor and the block itself. Thus changing the axial position of the shorting block is equivalent to modifying the load capacitance of line 2, that is, the inverter constant.

V. Experimental Results

In this section we present a few experimental results that were obtained by the above procedure from the microstrip lines shown in Fig. 11. These were made by thin-film technique on 99.5-percent alumina substrate (ε_r = 10.6) and had the following geometry:

strip width	0.5 mm
strip spacing	0.1 mm
substrate thickness	0.635 mm

The metal film was made of a 500-Å layer of NiCr plus a 1200-Å layer of gold (dc resistivity 2.7 $\mu\Omega \cdot$ cm). The latter was electrolytically grown to about 3 μm. The lengths of the even- and odd-mode resonators were 5 and 4.3 cm, respectively. Three samples of each resonator were made from the same mask. Fig. 12 is a picture of the jig used to perform the measurement. Also shown in the same figure is the stepped short-circuiting block that was used in the odd-mode case.

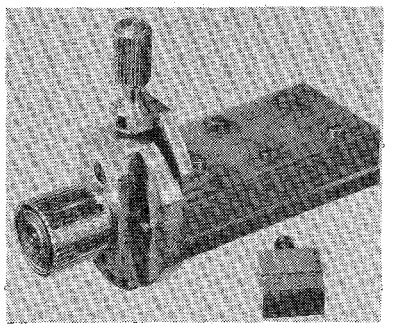

Fig. 12. Picture of jig used to perform measurements.

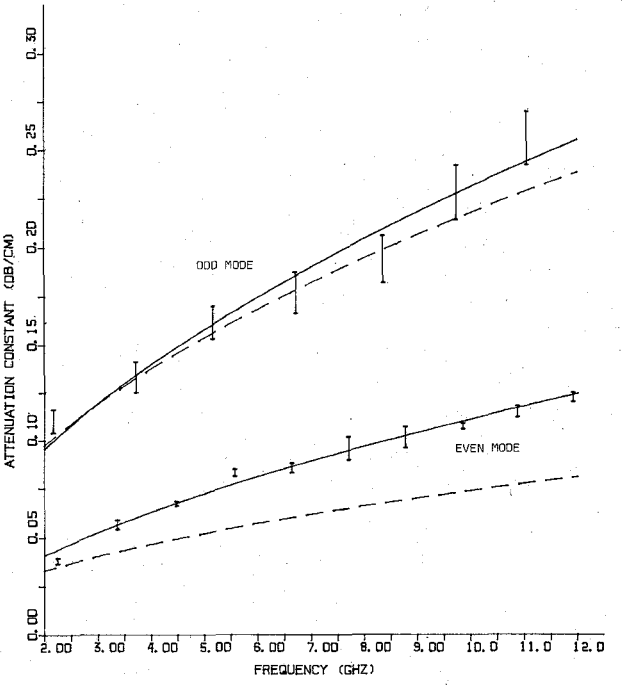

Fig. 13. Sample experimental results.

The measured performances of both the even and odd mode for all samples are reported altogether in Fig. 13. For each resonant frequency, an interval rather than a single measured point is given in the figure owing to the following reasons:

1) the attenuation constants are not exactly the same for the different resonators considered;
2) for each resonator there exists an uncertainty on the value of the loaded Q, arising from the irregular shape of the observed resonant dip.

On the other hand, practically no change of the resonant frequencies was found from one resonator to another. As is evident from the figure, measurement definition is good, the maximum uncertainty being about ± 6 percent both for the even and odd mode. The continuous curves were obtained by interpolating the midpoints of the uncertainty intervals in the least square sense. The interpolating function was chosen as

$$\alpha = Af^x$$

and the following values were found:

$$\begin{aligned} A &= 0.027 \\ x &= 0.615 \end{aligned} \quad \text{even mode}$$

$$\begin{aligned} A &= 0.066 \\ x &= 0.546 \end{aligned} \quad \text{odd mode}$$

where α is given in decibels per centimeter. Note that in both cases the exponent is higher than the theoretical 0.5, probably due to the effect of surface roughness [13].

Also shown in the figure are the results of loss computation for the same two-strip system (dashed lines). These may be expressed as

$$\alpha = 0.0234\sqrt{f} \quad \text{even mode}$$

$$\alpha = 0.0688\sqrt{f} \quad \text{odd mode}$$

where f is in gigahertz and the 1-GHz values were calculated by the quasi-TEM analysis of [14]. In each case the agreement is good at low frequencies, but deteriorates as frequency is increased, due to the exponent difference. The accuracy of the theoretical results is definitely better for the odd than for the even mode, but no simple explanation was found for this fact. Note that the calculations were performed for smooth strips and substrates; the agreement between theory and experiment could obviously be improved by including a roughness factor as in [4].

From Fig. 13 the resonant frequencies are also apparent, so that the even- and odd-mode phase velocities can be computed. For the even mode a slight dispersion effect is observed, since the phase velocity steadily decreases from 1.12×10^8 m/s (at 2 GHz) to 1.08×10^8 m/s (at 12 GHz). For the odd mode, dispersion is insignificant over the frequency range considered here, and the phase velocity has a practically constant value of 1.24×10^8 m/s. These results are consistent with those reported in [15].

For comparison, the velocity values obtained from the variational analysis of [16] for the same strip dimensions and zero thickness are

$$v_p = 1.103 \times 10^8 \text{ m/s} \quad \text{even mode}$$

$$v_p = 1.241 \times 10^8 \text{ m/s} \quad \text{odd mode.}$$

The maximum error of the quasi-TEM analysis on the even-mode velocity is about 2 percent below 12 GHz, while the odd-mode velocity is evaluated exactly.

Thus the quasi-TEM analysis seems adequate for characterizing the even and odd modes of symmetrical coupled microstrip lines up to 12 GHz, both for propagation velocity and losses. This conclusion was further checked by a number of measurements performed on rexolite resonators by the same technique described above. In all cases the results were qualitatively similar to those reported in the present section.

VI. Conclusion

In the present paper the theory of resonance measurements on lossy one-port networks has been formalized and presented in a general and self-contained form, independent of the physical nature of the particular circuit being considered. The basic equations to be used when measuring transmission-line propagation constants have been shown to be a simple and natural consequence of the general ones, for the special case of a network consisting of a short- or open-circuited transmission-line section.

Application of the general considerations to MIC transmission-line measurement has then been discussed. Particular attention has been devoted to such details as evaluation of the effects of dispersion, and the accuracy of the method has been established via computer simulation. Also, it has been shown that the measurement of even- and odd-mode propagation constants in coupled microstrips can easily be reduced to a couple of independent single-line measurements. The shape of the samples required to perform the measurement this way (see Fig. 11) is much simpler than for previously described methods (e.g., [15]), and a simple means of tuning the cavity without changing the circuit configuration is always available. As a consequence, measurements are much easier to be carried out and give better-defined and more repeatable results.

Finally, measured and computed data have been compared, and it has been shown that the quasi-TEM approximation (e.g., [14]) is reasonably adequate for computing even- and odd-mode attenuation constants up to 12 GHz.

Appendix

In this Appendix we show a procedure allowing the group velocity of a transmission-line resonator to be experimentally found [2]. Let the resonator be a short-circuited one and θ_s its electrical length at resonance. Then from (20),

$$\theta_s = (2K + 1)\frac{\pi}{2}. \tag{A1}$$

Now if the resonator length is changed by a small (known) amount Δl, the resonance frequency is also shifted by a corresponding amount $\Delta\omega_s$, but the electrical angle at resonance remains unchanged since it must satisfy (A1). On the other hand, we obviously have $\theta_s = \beta l|_{\omega=\omega_s}$, so that differentiating (A1) yields

$$\begin{aligned} 0 = \Delta\theta_s &= l\left.\frac{d\beta}{d\omega}\right|_{\omega=\omega_s}\Delta\omega_s + \beta\Big|_{\omega=\omega_s}\Delta l \\ &= \frac{l}{v_g}\Delta\omega_s + \frac{\omega_s}{v_p}\Delta l. \end{aligned} \tag{A2}$$

By means of (A2) the group velocity can be expressed as a function of known quantities and measured data:

$$v_g = -v_p\frac{\Delta\omega_s}{\omega_s}\frac{l}{\Delta l}. \tag{A3}$$

In this way the limitation pointed out by Pucel [4] may be overcome. In practice, two samples of the same line having slightly different lengths will be made and separately measured. In the open-resonator case, $2K + 1$ is replaced by $2K$ in (A1) and the same argument applies.

ACKNOWLEDGMENT

The author is indebted to Dr. Pirini of Telettra S.p.A. (Vimercate, Italy) for kindly making the microstrip lines described in Section V (see Fig. 11).

REFERENCES

[1] Y. Klinger, "The measurement of spurious modes in over-moded waveguides," *Proc. IEE*, vol. 106 B, Suppl. 13, pp. 89–93, 1959.
[2] F. Valdoni, "Misura a risonanza dell'accoppiamento tra modi diversi," *Note Recensioni e Notizie*, vol. XXII, no. 4, pp. 440–449, July 1973.
[3] M. Sucher and J. Fox, *Handbook of Microwave Measurement*, vol. I, 3rd ed. New York: Polytechnic Press, 1963, pp. 359–363.
[4] R. A. Pucel, D. J. Massé, and C. P. Hartwig, "Losses in microstrip," *IEEE Trans. Microwave Theory Techn.*, vol. MTT-16, pp. 342–350, June 1968.
[5] P. Troughton, "Measurement techniques in microstrip," *Electronics Letters*, vol. 5, pp. 25–26, Jan. 23, 1969.
[6] J. H. C. Van Heuven, "Conduction and radiation losses in microstrip," *IEEE Trans. Microwave Theory Techn.*, vol. MTT-22, pp. 841–844, Sept. 1974.
[7] G. C. Corazza and F. Valdoni, "Bipoli Stazionari," *Alta Frequenza*, vol. XLII, pp. 22–26, Jan. 1973.
[8] G. C. Corazza *et al.*, "Multiporte Stazionari," *Alta Frequenza*, vol. XLII, pp. 27–31, Jan. 1973.
[9] V. Rizzoli, "Resonance measurement of even- and odd-mode propagation constants in coupled microstrips," in *IEEE MTT-S International Microwave Symposium Digest* (Palo Alto, CA, May 1975), pp. 106–108.
[10] W. J. Getsinger, "Microstrip dispersion model," *IEEE Trans. Microwave Theory Techn.*, vol. MTT-21, pp. 34–39, Jan. 1973.
[11] J. S. Wight *et al.*, "Equivalent circuits of microstrip impedance discontinuities and launchers," *IEEE Trans. Microwave Theory Techn.* (Short Papers), vol. MTT-22, pp. 48–52, Jan. 1974.
[12] J. Wolff and W. Menzel, "The microstrip double ring resonator," *IEEE Trans. Microwave Theory Techn.*, vol. MTT-23, pp. 441–444, May 1975.
[13] *Advances in Microwaves*, Leo Young, Ed., vol. 8. New York: Academic Press, 1974.
[14] V. Rizzoli, "Losses in microstrip arrays," *Alta Frequenza*, vol. XLIV, pp. 86–94, Feb. 1975.
[15] J. G. Richings and B. Easter, "Measured odd- and even-mode dispersion of coupled microstrip lines," *IEEE Trans. Microwave Theory Techn.*, vol. MTT-23, pp. 826–828, Oct. 1975.
[16] V. Rizzoli, "A unified variational solution to microstrip array problems," *IEEE Trans. Microwave Theory Techn.*, vol. MTT-23, pp. 223–235, Feb. 1975.

A Dual Mode Tuning Circuit for Microwave Transistor Oscillators

ROBERT G. ROGERS, MEMBER, IEEE

Abstract—**A two-port circuit adjusting both even and odd mode fields, with orthogonal mode adjustment, can be used as an embedding circuit for a microwave transistor oscillator. The circuit, analyzed in TEM line, may also be realized in any other form of transmission line geometry, including two coexistent modes in a cavity. The resulting oscillator is stable, has low FM noise, and is readily tunable. Analyses of the tuning circuit and oscillator are presented, along with some experimental results and a discussion of methods using other than TEM transmission lines to produce the even and odd modes.**

I. INTRODUCTION

MICROWAVE transistors vary sufficiently in characteristics between manufacturers and within a type number that an effective oscillator is difficult to obtain satisfying the stringent conditions usually imposed by system requirements.

The transistor embedding circuit described here provides a feedback circuit for a microwave transistor, giving high-quality performance over a good bandwidth. The half-wavelength series element in the tuning circuit serves as the frequency-determining portion of the embedment, and is effectively isolated from the active element, giving frequency stability and low FM noise to the oscillator. The two tuning adjustments of the embedment allow relatively constant power output over a wide tuning range, without further output tuning.

Even and odd mode fields are separately adjusted at the transistor ports to give optimum conditions for oscillation. These fields may be TEM, as presented here, or from higher order modes in stripline, rectangular, cylindrical, or coaxial waveguide.

Manuscript received December 19, 1975; revised July 23, 1976.
The author is with GTE Lenkurt, Inc., San Carlos, CA 94070.

II. THE TUNING NETWORK

Fig. 1 shows the network, considered as air dielectric microstrip above a ground plane. The length l_1 extends from the two ports to the short circuit across conductors; l_2 continues from this short circuit to the grounding of both conductors to the ground plane.

The TEM even and odd mode electric field distributions at the ports are shown in Fig. 2. The short circuit between conductors is odd mode; grounding of both conductors also forms an odd mode short but no odd mode field exists on length l_2. So the odd mode length is l_1 and is adjusted only by changing l_1.

The even mode length is $l_1 + l_2$ but is adjusted only by l_2. With both modes existing at once, it can be seen from Fig. 2 that since the field intensities at the two ports will